Journal of
Nanoscience and Nanotechnology
Vol. 13, 1–6, 2013

Synthesis and Characterisation of Polygonal Indium Tin Oxide Nanocrystals

Bon-Ryul Koo[1], Byung Kyu Park[2], Chang Yeoul Kim[3], Sung-Tag Oh[1], and Hyo-Jin Ahn[1,*]

[1] *Department of Materials Science and Engineering, Seoul National University of Science and Technology, Seoul 139-743, South Korea*
[2] *Korea Basic Science Institute Suncheon Center, Suncheon 540-742, South Korea*
[3] *Future Convergence Ceramic Division, Korea Institute Ceramic Engineering and Technology (KICET), Seoul 233-5, South Korea*

Polygon ITO (Sn-doped In_2O_3) nanocrystals were synthesised via electrospinning, and their morphology, structural properties, and chemical composition were characterized by X-ray diffraction (XRD), scanning electron microscopy (SEM), transmission electron microscopy (TEM), and X-ray photoelectron spectroscopy (XPS). To determine the optimum conditions for the fabrication of polygon ITO nanocrystals, calcination temperature after the electrospinning process was controlled at 500 °C, 600 °C, 700 °C, and 800 °C, and the amount of PVP polymer was controlled at 4 wt%, 7 wt%, and 10 wt%. For comparison purposes, single In_2O_3 nanocrystals were also synthesised via electrospinning and calcination. The results show that ITO nanocrystals fabricated at a calcination temperature of 800 °C and with 10 wt% of PVP polymer exhibit clear polygon structure with single-crystallinity, which may be explained in terms of the effect of Sn doping in the In_2O_3 matrix and the oriented aggregation and Oswald ripening growth during the fusion process of ITO nanocrystals.

Keywords: ITO, Single-Crystallinity, Polygon, Electrospinning.

RESEARCH ARTICLE

1. INTRODUCTION

Indium tin oxide (ITO, tin-doped indium oxide), which is a degenerate *n*-type semiconductor having a band gap in the range 3.5–4.3 eV, has recently been receiving considerable interest in the field of electronic and optoelectronic devices such as solar cells, liquid crystal displays, organic light-emitting devices (OLED), and antireflection coatings because of its unique properties such as high optical transmittance in the visible region and low resistivity.[1] Thus far, various synthetic methods for obtaining high-quality ITO films have been developed, namely, sputtering, spray pyrolysis, microwave-assisted synthesis, co-precipitation, hydrothermal, sol–gel, pulsed-laser deposition, and electrospinning.[2–9] Among these synthetic methods, electrospinning has been widely used to fabricate ITO nanowires for use in various applications. For example, Lin et al. reported the fabrication and electrical properties of well-aligned ITO nanowires via electrospinning. They revealed the optimum conditions for the fabrication and demonstrated the effect of Sn doping for achieving high conductivity of the nanowires.[9] Munir et al. investigated the sheet resistance dependence on the PEO/ITO ratio; ITO films with the optical transmittance in the visible region were prepared via electrospinning.[10] In addition, Iskandar et al. reported the use of an ITO nanowire film electrode with an average diameter of ∼200 nm for the fabrication of dye-sensitised solar cells having efficiency up to ∼3.97%.[11] In this context, it is well-known that an electrospinning method, which is cost effective, highly repeatable, and versatile method, has been generally used to fabricate one-dimensional (1-D) nanowires.[12–14] On the other hand, we successfully synthesised zero-dimensional (0-D) polygon ITO nanocrystals by using an electrospinning technique. Furthermore, a study on structural properties and formation mechanism of 0-D polygon ITO nanocrystals fabricated via electrospinning has not been reported hitherto.

In this study, polygon ITO nanocrystals were successfully fabricated via electrospinning under the optimum calcination temperature and amount of PVP polymer and their morphology, structural properties, and chemical composition were characterised.

*Author to whom correspondence should be addressed.

2. EXPERIMENTAL DETAILS

Polygon ITO nanocrystals were successfully fabricated via electrospinning as follows. Tin chloride dehydrate ($SnCl_2 \cdot 2H_2O$, Aldrich), indium chloride tetrahydrate ($InCl_3 \cdot 4H_2O$, Aldrich), ethanol (Alfa Aesar), *N*,*N*-Dimethylformamide (C_3H_7NO, DMF, Aldrich), and polyvinylpyrrolidone (PVP, M_w = 1,300,000 g/mol, Aldrich) were used for preparing the precursor solution for electrospinning. The molar ratio of indium and tin was fixed at 9:1. First, the indium precursor was dissolved in ethanol solution by stirring the solution using a magnetic bar for 0.5 h. Subsequently, the tin precursor was dissolved in the mixture solution of the indium precursor and ethanol for 0.5 h. Then, PVP polymer was dissolved in a solvent consisting of DMF and ethanol solution for 1 h. Finally, a PVP-based solution was mixed into the above-dispersed solution for 1 h. The distance between the needle tip and the collector was fixed at ~ 10 cm and the feeding rate was controlled at 0.02 ml/h under an applied voltage of 14 kV. Thus, as-spun nanofibers (NFs) consisting of precursors and PVP polymer composite were fabricated. To investigate morphology and crystallinity, four samples were fabricated at calcination temperatures of 500 °C, 600 °C, 700 °C, and 800 °C (referred to here as sample A, sample B, sample C, and sample D, respectively) for 5 h and the amount of PVP polymer was controlled at 4 wt%, 7 wt%, and 10 wt%. As a result, 0-D polygon ITO nanocrystals were obtained via electrospinning under the optimum calcination temperature and amount of PVP polymer.

The crystallinities and structural properties of all the samples were characterised by X-ray diffraction (XRD, Rigaku X-ray diffractormeter equipped with a Cu Kα radiation) in the range of 10° to 80°. The morphologies and crystalline structures of the samples were investigated by scanning electron microscopy (SEM, Hitachi S-4700) and high-resolution electron microscopy (HREM, JEOL, 2100F, KBSI Suncheon center) analyses. The chemical bonding states and composition of all the samples were determined by performing X-ray photoelectron spectroscopy (XPS, ESCALAB 250 equipped with an Al Kα X-ray source).

3. RESULTS AND DISCUSSION

An electrospinning apparatus is composed of three components, namely a high voltage power supply, a syringe pump, and a grounded collector, as shown in Scheme 1(a). It is well-known that an electrical charge induced from a high voltage power supply is used in order to obtain nano-sized fibers from a liquid into a syringe. Scheme 1(b) shows as-spun NFs, consisting of precursor and polymer composite NFs, obtained from a grounded collector before calcination. After the calcination of as-spun NFs, an electrospinning technique is generally used to fabricate 1-D NFs. However, in this study, we successfully fabricated 0-D ITO nanocrystals via electrospinning, as shown in Scheme 1(c).

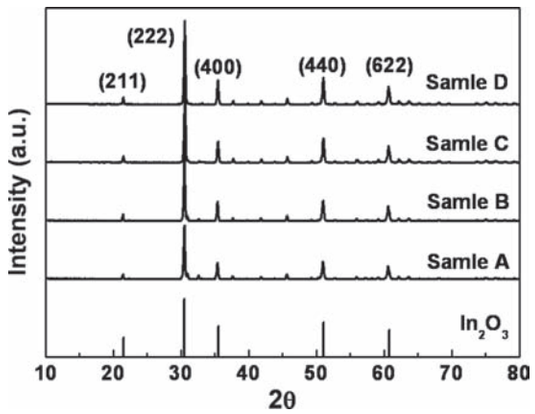

Fig. 1. XRD data of samples A, B, C, and D obtained after calcination.

Figure 1 shows XRD plots of samples A, B, C, and D obtained at calcination temperatures of 500 °C, 600 °C, 700 °C, and 800 °C, respectively. The main characteristic diffraction peaks of all the samples are observed at 21.60°, 30.69°, 35.50°, 51.09°, and 60.80°, corresponding to the (211), (222), (400), (440), and (622) planes of the body-cantered cubic structure of In_2O_3 (space group Ia3 [206]), respectively (JCPDS card No. 06-0416). It is interesting to note that all diffraction peaks slightly shifted toward high angles compared to the pure cubic In_2O_3 (i.e., $2\theta = 30.5°$ for the (222) plane). This result implies the replacement of the Sn ion in the In_2O_3 lattice. That is, because the ionic radius of Sn^{4+} (0.069 nm) is smaller than that of In^{3+} (0.08 nm), the ITO lattice is the smaller than the cubic In_2O_3 lattice, which can be explained using the Bragg equation ($\lambda = 2d \sin\theta$). This will be discussed in detail later in this section. Thus, we successfully fabricated ITO nanocrystals having a body-centred cubic structure. In addition, compared to other samples, sample D

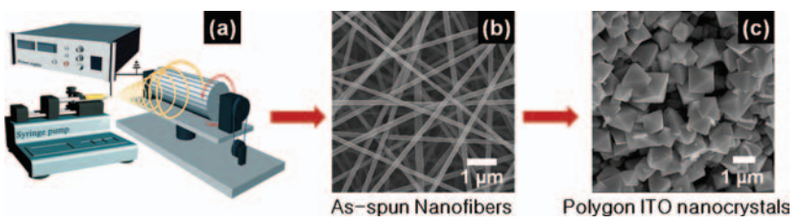

Scheme 1. A schematic diagram for a fabrication procedure of the polygonal ITO nanocrystals.

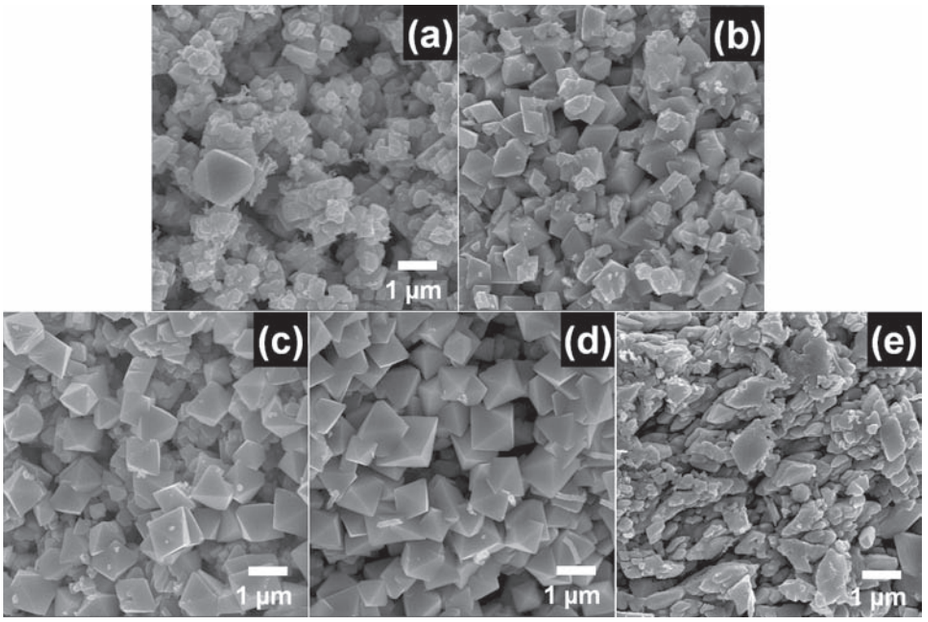

Fig. 2. SEM images of (a) sample A, (b) sample B, (c) sample C, (d) sample D, and (e) the single In_2O_3 nanostructures obtained after calcination.

fabricated at 800 °C exhibits a higher diffraction intensity and excellent crystallinity of the ITO nanocrystals.

Figure 2 shows SEM images of samples A, B, C, D, and single In_2O_3. Calcination temperature of samples A, B, C, D, and single In_2O_3 was controlled at 500 °C, 600 °C, 700 °C, 800 °C, and 800 °C, respectively. The diameter of the samples ranged from ∼280 nm to ∼1400 nm for sample A, ∼450 nm to ∼1020 nm for sample B, ∼740 nm to ∼1140 nm for sample C, and ∼890 nm to ∼1840 nm for sample D. Thus, as the calcination temperature was increased from 500 °C to 800 °C, the diameter of ITO gradually increased. In particular, it is noted that the morphology of ITO nanocrystals at 800 °C reveals a clear polygonal structure due to the oriented aggregation and Oswald ripening growth during the fusion process of ITO nanocrystals.[15] For comparison purposes, the single In_2O_3 was synthesised via electrospinning and calcined under the same experimental condition. As shown in Figure 2(e), the

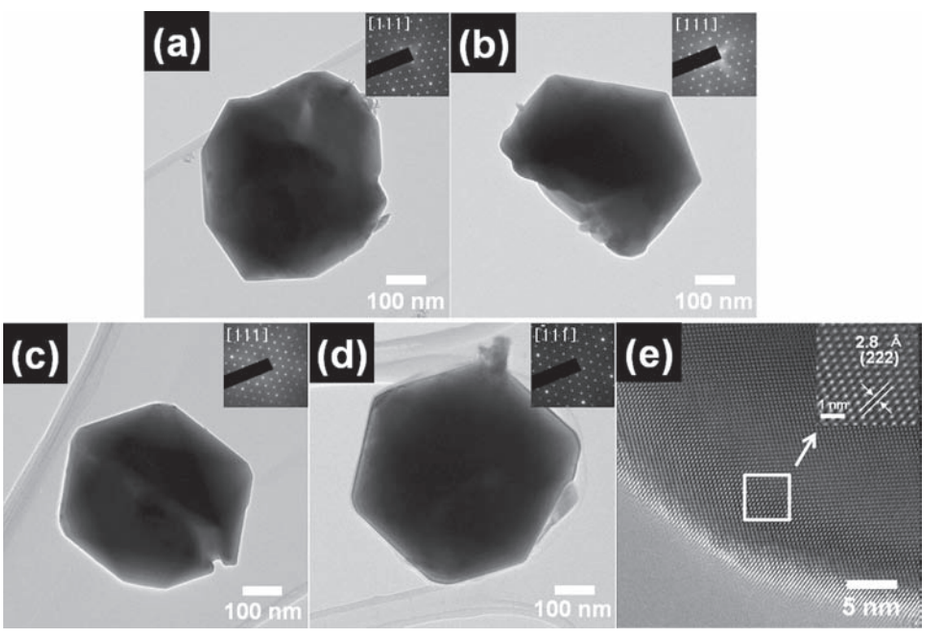

Fig. 3. TEM images and EDP data of (a) sample A, (b) sample B, (c) sample C, (d) sample D, and (e) the enlarged TEM images obtained from sample D.

RESEARCH ARTICLE

morphology of the single In_2O_3 exhibits irregular shaped structures. Therefore, the successful formation of polygon ITO nanostructures may be attributed to the doping effect of the Sn ion with calcination at 800 °C. The suppression of the Sn ion doped in the In_2O_3 matrix appears to affect the formation of polygonal ITO nanostructures during calcination.

Figures 3(a)–(d) show TEM images and electron diffraction patterns (EDP) of samples A, B, C, and D after calcination. These results show that the morphology from sample A to sample D changed gradually from an irregular shape to a polygonal shape. The morphologies of the samples in the TEM observations are in good agreement with the above SEM observations. Interestingly, EDP (the top right) consists of clear spots along the [111] zone around the (000) spot, which shows the single-crystalline properties. Furthermore, the EDP data exhibit [111] diffraction patterns of a general cubic structure. To further investigate the structural properties, enlarged HRTEM images of sample D (Fig. 3(d)) were obtained, as shown in Figure 3(e). These images show that atoms are uniformly and regularly distributed in the polygonal ITO nanocrystals. It is well-known that the lattice distance of the (222) plane for single In_2O_3 is 2.912 Å. However, the lattice distance of the (222) plane of the polygonal ITO nanocrystals is clearly observed to be $\sim$2.8 Å, as shown in the inset of Figure 3(e). Thus, polygonal ITO nanocrystals having single-crystalline structures were successfully fabricated via electrospinning because of their smaller lattice distance when compared to the single In_2O_3 materials.

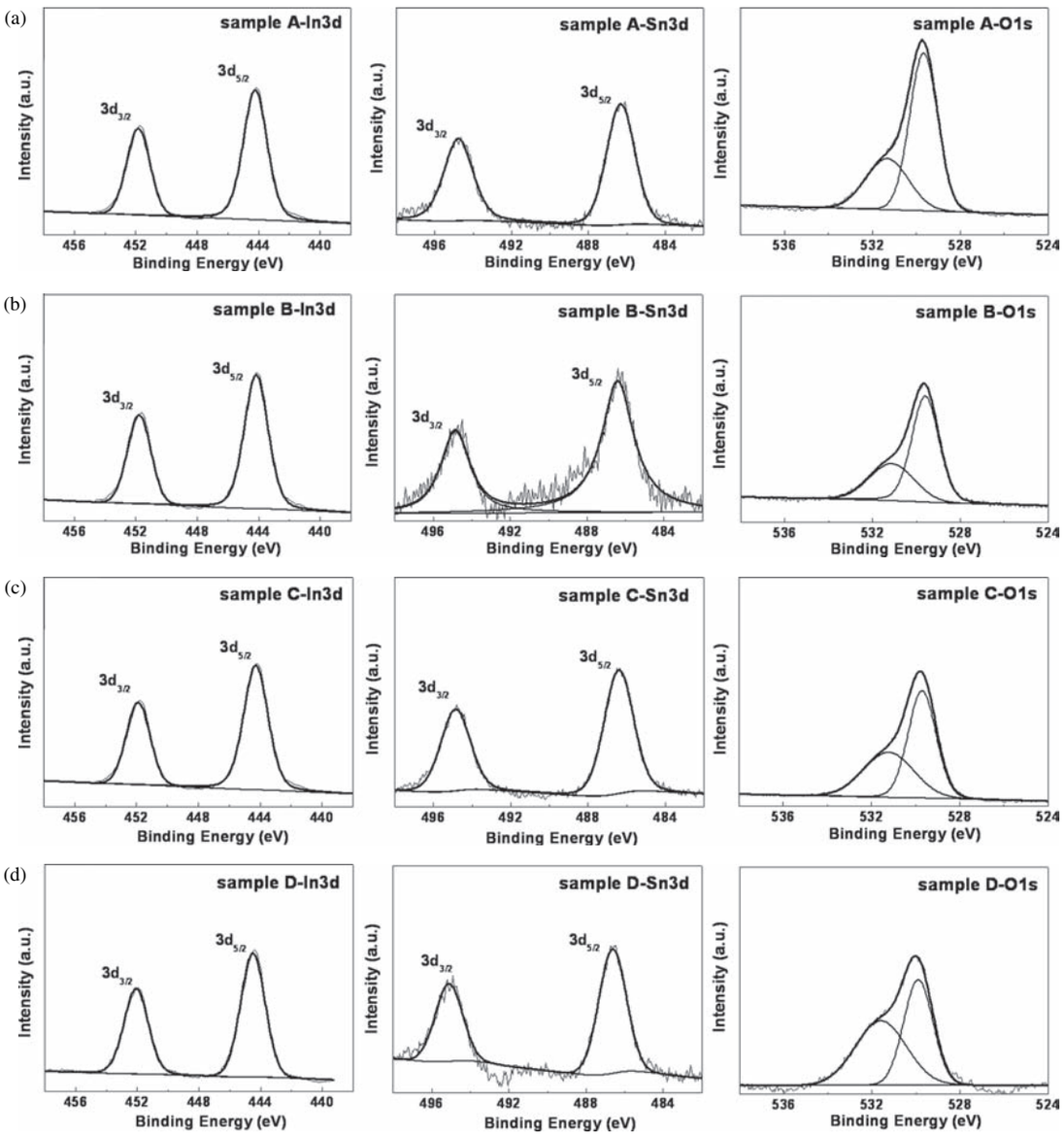

Fig. 4. XPS core-level spectra obtained from the In 3*d*, Sn 3*d*, and O 1s for samples A, B, C, and D.

RESEARCH ARTICLE

To examine the chemical bonding state of In and Sn, XPS measurement was performed on the four samples. For charge correction, the peak of the C 1s line (284.5 eV) was used as a reference. Figure 4 presents XPS core-level spectra of the In 3d, Sn 3d, and O 1s obtained from samples A, B, C, and D after calcination. For samples A, B, and C, the XPS core-level spectra for In $3d_{5/2}$ and In $3d_{3/2}$ photoelectrons were observed at ∼444.2 and ∼451.8 eV, respectively, and those for the Sn $3d_{5/2}$ and Sn $3d_{3/2}$ photoelectrons were observed at ∼486.4 and ∼494.9 eV, respectively. These results imply that elemental In and Sn were formed as In_2O_3 and SnO_2, which is in agreement with the results reported in the literature.[16] For sample D, the XPS core-level spectra for In $3d_{5/2}$ and In $3d_{3/2}$ photoelectrons were observed at ∼444.5 and ∼452.1 eV, respectively, and those for Sn $3d_{5/2}$ and Sn $3d_{3/2}$ photoelectrons were observed at ∼486.6 and ∼495.1 eV, respectively. Thus, the binding energy of the polygon ITO nanocrystals slightly shifted to higher values compared to a pure SnO_2 and In_2O_3 sample, owing to the doping effect of the Sn ion in the In_2O_3 matrix. Moreover, the XPS spectra for the O 1s of the samples was observed at ∼529.7 eV for O 1s-In and ∼531.2 eV for O 1s-Sn. This implies that the polygonal ITO nanocrystals consist of In_2O_3 and SnO_2 phases. Thus, the XRD, SEM, TEM, and XPS results indicate the successful synthesis of polygonal ITO nanocrystals via electrospinning.

To further investigate the formation mechanism of polygon ITO nanocrystals, we used three different amounts of PVP polymer, namely 4 wt%, 7 wt%, and 10 wt%, at a calcination temperature of 800 °C for 5 h, as shown in Figure 5(a). Polygonal ITO nanocrystals fabricated using 4 wt% (Fig. 5(b)) and 7 wt% of PVP polymer (Fig. 5(c)) were not as well formed as those fabricated using 10 wt% of PVP polymer (Fig. 2(d)). This implies that the optimum amount (10 wt%) of PVP polymer played a key role in the formation of the polygonal ITO nanocrystals. That is, a higher PVP concentration exhibits the effect of the superior stabilizer for synthesizing the polygon ITO nanocrystals.[17] Previously, 1-D inorganic nanowires were fabricated at a calcination temperature of ∼400 °C.[18, 19] However, at a calcination temperature of up to 800 °C, 1-D inorganic nanowires cannot be fabricated because of the large grain growth in the as-spun 1-D nanowires. Thus, 0-D inorganic nanocrystals will be formed. In our study, polygonal ITO nanocrystals were successfully formed at a calcination temperature of 800 °C with the optimum amount (10 wt%) of PVP polymer. Under these conditions, the polygonal morphology of the ITO nanocrystals is well formed. As a result, the possible formation mechanism of polygon ITO nanocrystals is explained in terms of the doping effect of the Sn ion in the In_2O_3 matrix and the fusion of ITO nanocrystals due to the oriented aggregation and Oswald ripening growth under the optimum experimental conditions.

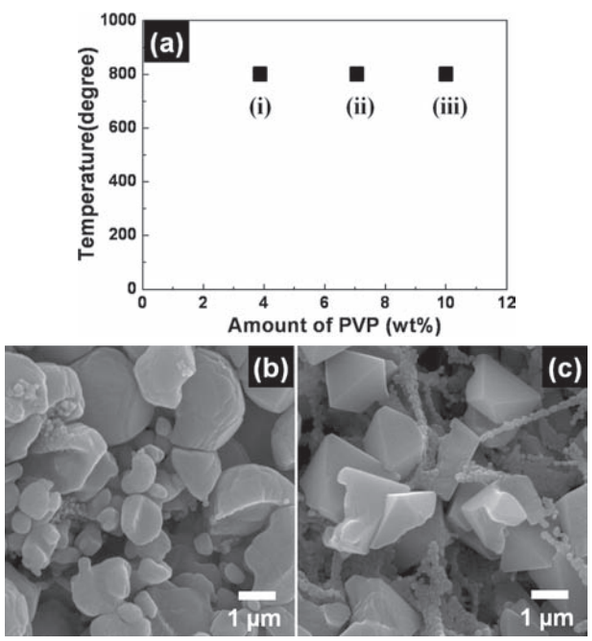

Fig. 5. The amount dependence of PVP polymer with calcination temperature at 800 °C.

4. CONCLUSIONS

Polygon ITO nanocrystals were fabricated via electrospinning, and their morphology, structural properties, and chemical composition were characterised by XRD, SEM, TEM, and XPS analyses. The results of the analyses indicate that after calcination at 800 °C, the ITO nanocrystals show a clear polygonal morphology with a single-crystalline property. Therefore, the successful formation of polygon ITO nanocrystals could be explained by the synergy effects resulting from the doping effect of the Sn ion in In_2O_3 and the oriented aggregation and Oswald ripening growth during the fusion process of ITO nanocrystals under the optimum experimental conditions such as the calcination temperature of 800 °C and the amount (10 wt%) of PVP polymer.

Acknowledgments: This work was supported by Grant No. 10041161 from the Ministry of Knowledge Economy (MKE) and the Fundamental R&D Program for Core Technology of Materials funded by the Ministry of Knowledge Economy, Republic of Korea.

References and Notes

1. J. Liu, D. Wu, and S. Zeng, *J. Mater. Process. Tech.* 209, 3943 (**2009**).
2. R.N. Joshi, V.P. Singh, and J.C. McClure, *Thin Solid Films* 257, 32 (**1955**).
3. S.M. Rosati, and T. Ganj, *Renew. Energy* 29, 1671 (**2004**).
4. G. Buhler, D. Tholmann, and C. Feldmann, *Adv. Mater.* 19, 2224 (**2007**).

RESEARCH ARTICLE

5. V. Senthilkumar, K. Senthil, and P. Vickraman, *Mater. Res. Bull.* 47, 1051 **(2012)**.
6. H. R. Xu, H. Zhou, G. Zhu, J. Chen, and C. Liao, *Mater. Lett.* 60, 983 **(2006)**.
7. M. J. Alam and D. C. Cameron, *Thin Solid Films* 420, 76 **(2002)**.
8. X. T. Ren, M. B. Huang, S. Amadon, W. A. Lanford, M. A. Morales Paliza, and L. C. Feldman, *Nucl. Instrum. Meth. B* 174, 187 **(2001)**.
9. D. Lin, H. Wu, R. Zhang, and W. Pan, *Nanotechnology* 18, 465301 **(2007)**.
10. M. M. Munir, F. Iskandar, K. M. Yun, K. Okuyama, and M. Abdullah, *Nanotechnology* 19, 145603 **(2008)**.
11. F. Iskandar, A.B. Suryamas, M. Kawabe, M. M. Munir, K. Okuyama, T. Tarao, and T. Nishitani, *Jpn. J. Appl. Phys.* 49, 010213 **(2010)**.
12. S. I. Noh, D. W. Park, H. S. Shim, and H. J. Ahn, *J. Nanosci. Nanotechnol*. 12, 6065 **(2012)**.
13. K. R. V. Subramanian, and A. Balakrishnan, *J. Nanosci. Nanotechnol*. 12, 7963 **(2012)**.
14. F. Yao, H. S. Wang, and G. D. Fu, *J. Nanosci. Nanotechnol*. 12, 7284 **(2012)**.
15. H. Li, T. Arita, S. Takami, and T. Adschiri, *Prog. Cryst. Growth Ch.* 57, 117 **(2011)**.
16. J. F. Moulder, W. F. Stickle, P. E. Sobol, and K. D. Bomben, Handbook of X-Ray Photoelectron Spectroscopy, Physical Electronics, Physical Electronics Inc., Eden Pairie **(1995)**, pp. 124–127.
17. R. Pan, S. Qiang, K. Liew, Y. Zhao, R. Wang, and J. Zhu, *Powder Technol.* 189, 126 **(2009)**.
18. G.-H. An. S.-Y. H Jeong, T.-Y. Seong, and H.-J. Ahn, *Mater. Lett.* 65, 2377 **(2011)**.
19. J.-B Lee, S.-Y. Jeong, W.-J. Moon, T.-Y. Seong, and H.-J. Ahn, *J. Alloy. Compd.* 509, 4336 **(2011)**.

Received: 1 May 2012. Accepted: 20 December 2012.

RESEARCH ARTICLE